JACS
JOURNAL OF THE AMERICAN CHEMICAL SOCIETY
Article
pubs.acs.org/JACS

# Energetics of Lipid Binding in a Hydrophobic Protein Cavity

Lan Liu,[†] Klaus Michelsen,[‡] Elena N. Kitova,[†] Paul D. Schnier,[‡] and John S. Klassen*[,†]

[†]Alberta Glycomics Centre and Department of Chemistry, University of Alberta, Edmonton, Alberta, Canada T6G 2G2
[‡]Molecular Structure, Amgen, Thousand Oaks, California 91320, United States

Supporting Information

**ABSTRACT:** Hydrophobic bonding is central to many biochemical processes, such as protein folding and association. However, a complete description of the forces underlying hydrophobic interactions is lacking. The goal of this study was to evaluate the intrinsic energetic contributions of $-CH_3$, $>CH_2$, and $-HC{=}CH-$ groups to protein−lipid binding. To this end, Arrhenius parameters were measured for dissociation of gaseous deprotonated ions (at the −7 charge state) of complexes of bovine *β*-lactoglobulin (Lg), a model lipid-binding protein, and a series of saturated, unsaturated, and branched fatty acids (FA). In the gas phase, the $(Lg + FA)^{7-}$ ions adopt one of two noninterconverting structures, which we refer to as the *fast* and *slow* dissociating components. The dissociation activation energies measured for the *fast* components of the $(Lg + FA)^{7-}$ ions were found to correlate linearly with the association free energies measured in aqueous solution, suggesting that the specific protein−lipid interactions are preserved in the gas phase. The average contributions that the $-CH_3$, $>CH_2$, and $-HC{=}CH-$ groups make to the dissociation activation energies measured for the *fast* components of the $(Lg + FA)^{7-}$ ions were compared with enthalpies for the transfer of hydrocarbons from the gas phase to organic solvents. For $>CH_2$ groups, the interior of the cavity was found to most closely resemble the relatively polar solvents acetone and *N*,*N*-dimethylformamide, which have dielectric constants ($\varepsilon$) of 21 and 39, respectively. For $-CH_3$ groups, the solvent environment most closely resembles 1-butanol ($\varepsilon$ = 17), although the energetic contribution is dependent on the location of the methyl group in the FA. In contrast, the solvation of $-HC{=}CH-$ groups is similar to that afforded by the nonpolar solvent cyclohexane ($\varepsilon$ = 2).

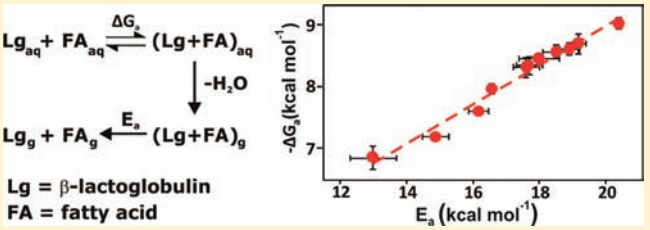


## INTRODUCTION

Hydrophobic bonding, which refers to the attraction of nonpolar molecules in water, plays a key role in many important biological processes.[1,2] For example, hydrophobic interactions are believed to be the major driving force for the folding of globular proteins, they are implicated in the assembly of proteins, and they are responsible for the noncovalent association of proteins with nonpolar molecules.[3] While the importance of hydrophobic bonding in biochemical reactions is well recognized and has been extensively investigated, a complete and quantitative description of the underlying forces is currently lacking.[3b,c] The phenomenon of hydrophobic bonding is often explained in terms of a large entropic factor resulting from the release of water molecules from the nonpolar surfaces of the solute molecules and their return to bulk solution.[3c,4] According to this view, the enthalpies for the interactions that are broken (water−solute) are similar in magnitude to those that are made (water−water and solute−solute), and consequently, enthalpy changes do not contribute appreciably to the free energy of association.[4] However, this simplistic view does not satisfactorily account the thermodynamic parameters reported for the association of many hydrophobic protein−protein and protein−ligand complexes.[5] Indeed, as noted by Lazardis,[5a] Dill,[5b] and others,[6] hydrophobic bonding may be primarily enthalpic or entropic in nature, depending on the structures of the binding partners and the solution conditions.

The thermodynamic contributions that hydrophobic interactions make to biochemical reactions, such as protein−ligand binding, are commonly estimated from thermochemical data tabulated for the transfer of small, nonpolar nonelectrolytes from water to nonaqueous solvents.[4] However, this approach—the use of small molecule transfer data applied in an additive fashion—to quantitatively describe the role of hydrophobic bonding in biochemical reactions suffers from a number of limitations.[4] For example, the premise that thermodynamic quantities measured for simple structures, for example, amino acids, can simply be added together to describe the properties of more complicated molecules, for example, proteins, has not been rigorously demonstrated.[4,7] The treatment of a biochemical system, such as the ligand binding site of a protein, as a homogeneous medium that can be represented as a single solvent type is likely overly simplistic.[4] Furthermore, experimental data, which could guide the selection of appropriate solvents to represent the ligand binding site, are absent.

By its very nature, hydrophobic bonding requires the presence of water. Nevertheless, new insights into the

Received: September 21, 2011
Published: January 12, 2012

   dx.doi.org/10.1021/ja208909n | J. Am. Chem. Soc. 2012, 134, 3054−3060

energetics of these interactions may be gained by interrogating hydrophobic protein complexes in the absence of water, that is, in the gas phase. In many cases, gas phase ions of intact noncovalent protein complexes, including those involving hydrophobic interactions, are readily produced by preforming the complexes in aqueous solution and transferring them to the gas phase using electrospray ionization (ESI).[8−13] In some cases, the addition of detergent micelles or organic solvents is necessary to solubilize the complexes and facilitate their transfer to the gas phase by ESI.[11] The use of stabilizing additives, such as imidazole, may also be required to prevent dissociation of the complexes during the ESI process.[14] Once in the gas phase, the structure and stability of the desolvated ions of the protein complexes may be probed using a variety of mass spectrometry (MS) techniques, such as ion dissociation reactions,[15] ion mobility,[16] or spectroscopic measurements.[17]

The interactions between bovine $\beta$-lactoglobulin (Lg) and fatty acids (FA) represent attractive model systems for studying the energetics of protein−lipid binding. Lg, an 18 kDa water-soluble whey protein, exists predominantly as a homodimer at physiological pH, and as monomer at pH >8.[18] The protein consists of nine $\beta$ strands (designated A−I), of which the A to H strands form an up-and-down $\beta$-barrel, and one major $\alpha$-helix.[19] The $\beta$-barrel forms a large and flexible cavity lined with 14 hydrophobic residues, with two basic residues located at the entrance of cavity. The flexible EF loop forms a lid over the entrance of the cavity; under basic conditions, the lid "opens" and allows ligands access to the cavity.[18,19] Notably, it has been reported that the cavity remains dry in the absence of bound ligand.[20] Consequently, water displacement from the protein cavity is not expected to contribute to the thermodynamics of ligand binding.

A variety of water-insoluble and weakly soluble ligands, including long chain FAs, are known to bind to Lg.[21] It was recently shown by ESI−MS that complexes of Lg and linear FAs, $CH_3(CH_2)_xCOOH$ where $x \geq 12$, can be transferred from aqueous solution to the gas phase with little or no dissociation.[13,22] Kinetic data for the loss of neutral FA from the deprotonated $(Lg + FA)^{7-}$ ion, together with the results of molecular dynamics (MD) simulations, provide evidence that the acyl chain of the FA is retained within the hydrophobic ligand binding cavity of Lg in the gas phase.[13] Furthermore, the dissociation mechanism of the deprotonated (Lg + FA) ions likely entails a late transition state (*TS*), wherein the ligand is almost completely removed from the binding pocket, such that the dissociation activation energy ($E_a$) provides a quantitative measure of the strength of the protein−lipid intermolecular interactions in the gas phase.[13,23]

The ability to preserve (Lg + FA) complexes in the gas phase and to quantify the intermolecular interactions offers an unprecedented opportunity to directly investigate the energetic contributions of individual functional groups and amino acid residues to hydrophobic bonding and to develop a more complete description of the interplay between intrinsic interactions and solvent effects in hydrophobic bonding. In the present study, we have, for the first time, evaluated the energetic contribution of $-CH_3$, $>CH_2$, and $-HC{=}CH-$ groups to protein−lipid binding in the gas phase. Arrhenius parameters were established for the dissociation of the deprotonated gaseous ions of complexes of Lg and a series of ligands (L) comprising branched and unsaturated FAs, as well as retinoic acid and retinol (Figure 1). From an analysis of the $E_a$ values determined in the present study and previously,[13] the

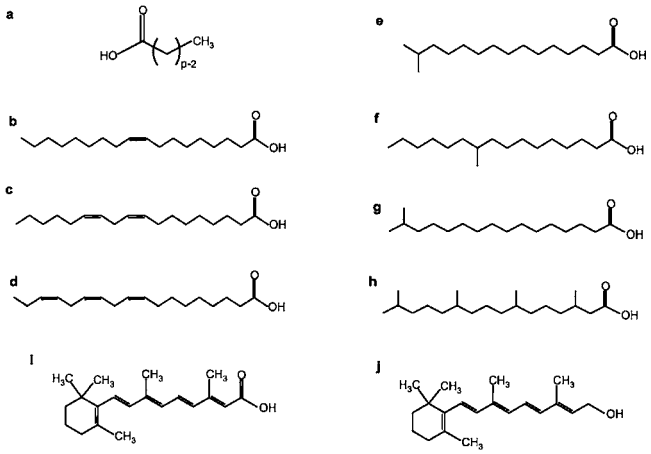


**Figure 1.** Ligand structures: (a) saturated fatty acids, lauric acid (LA, number of carbon atoms (nca) = 12), myristic acid (MA, nca = 14), palmitic acid (PA, nca = 16), stearic acid (SA, nca = 18); (b) oleic acid (SA-1, nca = 18); (c) linoleic acid (SA-2, nca = 18); (d) linolenic acid (SA-3, nca = 18); (e) isopalmitic acid (iPA, nca = 16); (f) 10-methylhexadecanoic acid (10-MePA, nca = 17); (g) 15-methylhexadecanoic acid (15-MePA, nca = 17); (h) phytanic acid (PhA, nca = 20); (i) retinoic acid (RA, nca = 20); and (j) retinol (RO, nca = 20).

energetic contributions of the methylene and methyl groups, as well as double bonds, to the kinetic stabilities of the (Lg + L) complexes were established. A comparison of these energetic data with enthalpies reported for the transfer of hydrocarbons from the gas phase to various organic solvents[24−26] provides insights into the nature of the "solvent environment" afforded to lipids by the hydrophobic cavity of Lg. Additionally, linear relationships between the association free energies measured in solution and the free energies of activation and activation energies for the dissociation of the dehydrated complexes were established. The structural and mechanistic implications of these findings for FA binding to Lg in water are discussed.

## EXPERIMENTAL SECTION

**Methods.** *Proteins and Ligands.* Bovine $\beta$-lactoglobulin (Lg, monomer MW 18281 Da), oleic acid (SA-1, 282 Da), linoleic acid (SA-2, 280 Da), linolenic acid (SA-3, MW 278 Da), retinoic acid (RA, 300 Da), retinol (RO, 286 Da), isopalmitic acid (iPA, 256 Da), and phytanic acid (PhA, 312 Da) were purchased from Sigma-Aldrich Canada (Oakville, Canada). 10-Methylhexadecanoic acid (10-MePA, 270 Da) and 15-methylhexadecanoic acid (15-MePA, 270 Da) were purchased from Matreya (Brockville, Canada). Structures of ligands are listed in Figure 1. For the ESI−MS measurements, Lg was dissolved and exchanged directly into Milli-Q water, using an Amicon microconcentrator with a molecular weight cutoff of 10 kDa. The concentration of the Lg solution was determined by lyophilizing a known volume of the filtrate and measuring the mass of the protein. The protein stock solution was stored at −20 °C. The RO stock solution was prepared by dissolving RO into methanol. Other ligand stock solutions were prepared by dissolving each ligand into 25 mM aqueous ammonium acetate. The ESI solutions were prepared from stock solutions of protein and ligand. Imidazole (10 mM) was also added in order to protect the (Lg + L) complexes against in-source dissociation during ESI−MS analysis.[23] Aqueous ammonium hydroxide was added to adjust the pH of the ESI solution to 8.5.

*Mass Spectrometry.* All experiments were performed on a 9.4 T Apex II FTICR mass spectrometer (Bruker, Billerica, MA) equipped with a nanoflow ESI ion source. Complete details of the instrumental


dx.doi.org/10.1021/ja208909n | J. Am. Chem. Soc. 2012, 134, 3054−3060

and experimental conditions used for the BIRD measurements and the direct protein−ligand affinity measurements, as well as a description of how the kinetic and affinity data were analyzed, can be found elsewhere.[13,22]

*Surface Plasmon Resonance Spectroscopy.* Surface plasmon resonance experiments were performed with a Biacore T100 instrument (GE Healthcare). Reagents used were obtained from either Sigma-Aldrich or GE Healthcare. The immobilization buffer consisted of 10 mM 4-(2-hydroxyethyl)-1-piperazineethanesulfonic acid (Hepes) (pH 7.4), 150 mM NaCl, and 0.2 mM tris(2-carboxyethyl)phosphine (TCEP). Lg was immobilized onto a carboxymethyl dextran (CM5) chip using amine coupling chemistry at 25 °C. Surfaces were preconditioned by flowing a solution containing 100 mM HCl, 50 mM NaOH, and 0.5% (w/v) sodium dodecyl sulfate (SDS) at a flow rate of 100 $\mu$L min$^{-1}$. The surface was activated for 7 min using a mixture of *N*-hydroxysuccinimide (NHS) and 1-ethyl-3-[3-dimethylaminopropyl]carbodiimide hydrochloride (EDC) followed by an injection (~5 min) of 20 $\mu$g mL$^{-1}$ Lg in 10 mM sodium acetate (pH 4.0). Remaining activated groups were subsequently blocked with a 7 min injection of ethanolamine. With this approach, approximately 800−1800 RU of Lg was immobilized. The running buffer for FA:Lg kinetic measurements consisted of 25 mM tris(hydroxymethyl)aminomethane (Tris) pH 8.0, 1 mM TCEP, 0.2 mM 3-[(3-cholamidopropyl)dimethylammonio]-1-propanesulfonate (CHAPS), and 8% (v/v) methanol. Stock solutions of PA and SA were prepared and serial dilutions were performed in methanol. Diluted FAs were added to the running buffer to give a final methanol concentration of 8% (v/v). The FAs were injected over the Lg surface for 30 s association and the dissociation was monitored for 60 s at a flow rate of 80 $\mu$L min$^{-1}$. The sample analysis temperature was varied between 5 and 45 °C.

Data were processed using the Biacore T100 analysis software and Igor Pro (Wavemetrics, Inc.). Sensorgrams were corrected for systematic noise and baseline drift by subtracting the response of the reference spot, which was activated but not exposed to protein. The average response from blank injections was used to double-reference the binding data. The dissociation portions of the sensorgrams were de-spiked, binomially smoothed, and fitted to an exponential function to determine the dissociation rate constants.

*Molecular Dynamics Simulations.* MD simulations were performed using the InsightII program suite (Accelrys, San Diego, CA). The crystal structure of the (Lg + RA) complex (1GX9) was used for the initial geometry of the gas phase $(Lg + RA)^{7-}$ ion. The simulations were performed using the force field Discover CVFF (consistent valence force field). Nine different charge distributions were considered.[13] The energies of the desolvated ions were first minimized by the steepest gradient method (1000 iterations), followed by conjugate gradient method (10 000 iterations) using a 0.001 kcal mol$^{-1}$ Å$^{-1}$ convergence criterion. At the start of the simulation, the system was equilibrated at 300 K for 1 ps with a time step of 1 fs. After this period, production dynamics were performed for 2.5 ns and data were collected every 250 fs. Upon completion of the simulations, analysis of structural parameters was carried out. The geometric criteria used to establish H-bonds are: heavy atom (A) to heavy atom (B) distance ≤3.5 Å and H-bond angle (AHB) ≥150°. A distance ≤5.0 Å served as the criterion for hydrophobic interactions.[27]

## RESULTS AND DISCUSSION

Deprotonated gas phase ions of the (Lg + L) complexes, that is, $(Lg + L)^{n-}$ ions $n$ = 6−8, were produced by ESI from aqueous ammonium acetate solutions of Lg and L at pH 8.5 and 25 °C. Imidazole was also added to the solution to prevent dissociation of the complexes during the ESI desolvation process.[14] Thermal rate constants ($k$) for the dissociation of the gaseous $(Lg + L)^{7-}$ ions were determined from time-resolved BIRD measurements. At the reaction temperatures investigated, 28−87 °C, BIRD of the $(Lg + L)^{7-}$ ions proceeds exclusively by the loss of neutral L, eq 1:

$$(Lg + L)^{7-} \rightarrow Lg^{7-} + L \quad (1)$$

Natural log plots of the normalized abundance of the $(Lg + L)^{7-}$ ions versus time measured for each ligand investigated are shown in Figure S1, Supporting Information. In each case, the kinetic plots exhibit nonlinear behavior that can be described by a double exponential function, indicating the presence of two distinct structures. These findings are consistent with those reported recently for the dissociation of $(Lg + FA)^{7-}$ ions composed of lauric, myristic, palmitic, and stearic acid.[13] These ions were shown to adopt one of two noninterconverting structures, which we refer to as the *fast* and *slow* dissociating components, that is, $(Lg + FA)_f^{7-}$ and $(Lg + FA)_s^{7-}$ ions, respectively. According to the results of MD simulations, in both structures the acyl chain remains buried in the hydrophobic cavity.[13] The main structural difference between the *fast* and *slow* structures, identified from MD simulations, is the position of the flexible EF loop of Lg. In the $(Lg + FA)_f^{7-}$ ions, the loop is in an "open" position, such that the FA is stabilized predominantly by protein−lipid interactions. In the $(Lg + FA)_s^{7-}$ ions, the loop is in a "closed" position and H-bonds between the ligand carboxyl group and Lg also contribute to the stability of the complex. Given the structural similarities of the FAs considered here and those investigated previously,[13] it is reasonable to expect that similar structural differences are responsible for the double exponential kinetics observed in the present study.

Rate constants were determined for both the $(Lg + L)_f^{7-}$ and $(Lg + L)_s^{7-}$ ions, that is, $k_f$ and $k_s$, respectively, and the corresponding Arrhenius plots are shown in Supporting Information Figure S2. The Arrhenius parameters ($E_a$ and $A$) are listed in Table 1. In Figure 2, the $E_a$ values are plotted versus the total number of ligand carbon atoms, for both the *fast* and *slow* components. It can been seen that, with the exception of the $(Lg + RA)_f^{7-}$ and $(Lg + RO)_f^{7-}$ ions, there exists a linear relationship between $E_a$ and the number of carbon atoms for the $(Lg + L)_f^{7-}$ ions, wherein each carbon contributes 0.94 ± 0.05 kcal mol$^{-1}$ to the $E_a$. In contrast, no simple relationship is evident for the $(Lg + L)_s^{7-}$ ions. Furthermore, the $E_a$ value for a given $(Lg + L)_s^{7-}$ ion is, in each case, larger than the value for the corresponding $(Lg + L)_f^{7-}$ ion. This finding is consistent with the earlier proposal that the $(Lg + L)_s^{7-}$ ions are stabilized by both protein−lipid interactions and H-bonds.[13]

A recent study of the thermal dissociation kinetics of the $(Lg + FA)^{7-}$ ions, composed of linear, saturated FAs, revealed that the $E_a$ values measured for the $(Lg + FA)_f^{7-}$ ions increased almost linearly with the length of the acyl chain, with each $>CH_2$ group contributing 0.82 ± 0.04 kcal mol$^{-1}$ to the dissociation energy.[13] That the inclusion of the kinetic data acquired for the methylated and unsaturated FAs leads to a somewhat larger average energy contribution of each carbon (for the *fast* components) indicates that methyl groups and double bonds bind more strongly to Lg than do the methylene groups. The interaction energies of $-CH_3$ groups, relative to $>CH_2$ groups, were established from differences in the $E_a$ values measured for the methylated and nonmethylated, saturated FAs. Implicit in this analysis is the assumption that the $-CH_3$ groups contribute in an additive fashion to the $E_a$ values. For 10-MePA and 15-MePA, the methyl groups are found to

**Table 1. Arrhenius Parameters ($E_a$, $A$) Determined for the Dissociation of the Gaseous $(Lg + L)_f^{7-}$ and $(Lg + L)_s^{7-}$ Ions[a,b]**

| ligand | $E_a$ (kcal mol$^{-1}$) | $A$ (s$^{-1}$) |
|---|---|---|
| | *Fast* | |
| LA | 13.0 ± 0.7[b] | $10^{8.4\pm0.5}$ [b] |
| MA | 14.9 ± 0.4[b] | $10^{9.5\pm0.3}$ [b] |
| PA | 16.2 ± 0.3[b] | $10^{10.2\pm0.2}$ [b] |
| SA | 18.0 ± 0.6[b] | $10^{11.3\pm0.4}$ [b] |
| SA-1 | 18.5 ± 0.4 | $10^{11.4\pm0.3}$ |
| SA-2 | 18.9 ± 0.3 | $10^{11.8\pm0.2}$ |
| SA-3 | 19.2 ± 0.2 | $10^{12.0\pm0.1}$ |
| iPA | 16.6 ± 0.1 | $10^{10.6\pm0.1}$ |
| 10-MePA | 17.7 ± 0.4 | $10^{11.0\pm0.3}$ |
| 15-MePA | 17.6 ± 0.4 | $10^{11.1\pm0.2}$ |
| PhA | 20.4 ± 0.1 | $10^{12.8\pm0.1}$ |
| RA | 12.6 ± 0.2 | $10^{7.2\pm0.2}$ |
| RO | 12.5 ± 0.4 | $10^{7.9\pm0.3}$ |
| | *Slow* | |
| LA | 25.3 ± 0.9[b] | $10^{15.4\pm0.6}$ [b] |
| MA | 21.3 ± 1.0[b] | $10^{13.0\pm0.7}$ [b] |
| PA | 23.8 ± 0.9[b] | $10^{14.2\pm0.6}$ [b] |
| SA | 21.5 ± 0.5[b] | $10^{12.7\pm0.3}$ [b] |
| SA-1 | 22.0 ± 0.4 | $10^{12.7\pm0.3}$ |
| SA-2 | 20.2 ± 0.4 | $10^{11.7\pm0.3}$ |
| SA-3 | 21.7 ± 0.9 | $10^{12.5\pm0.6}$ |
| iPA | 21.9 ± 1.0 | $10^{13.0\pm0.8}$ |
| 10-MePA | 24.2 ± 1.0 | $10^{14.3\pm0.7}$ |
| 15-MePA | 23.5 ± 0.4 | $10^{14.0\pm0.3}$ |
| PhA | 27.1 ± 0.5 | $10^{16.2\pm0.3}$ |
| RA | 15.6 ± 0.6 | $10^{7.9\pm0.4}$ |
| RO | 20.0 ± 0.9 | $10^{11.8\pm0.6}$ |

[a]The reported errors are one standard deviation. [b]Values taken from ref 13.

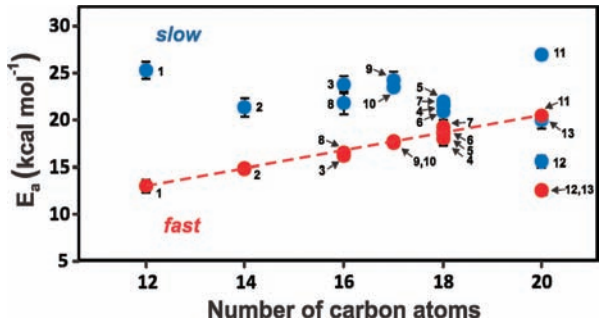


**Figure 2.** Plot of activation energies ($E_a$) measured for the dissociation of $(Lg + L)_f^{7-}$ (red circles) and $(Lg + L)_s^{7-}$ ions (blue circles), for L = LA (1), MA (2), PA (3), SA (4), SA-1 (5), SA-2 (6), SA-3 (7), iPA (8), 10-MePA (9), 15-MePA (10), PhA (11), RA (12), and RO (13) versus the number of carbons in L. The dashed line corresponds to linear least-squares fit of the $E_a$ values determined for all of the $(Lg + L)_f^{7-}$ ions, with the exception of the $(Lg + RA)_f^{7-}$ and $(Lg + RO)_f^{7-}$ ions.

contribute an additional 0.7 and 0.6 kcal mol$^{-1}$, respectively, to $E_a$. For PhA, the average contribution of the four $-CH_3$ groups is somewhat smaller, 0.3 kcal mol$^{-1}$ each. A similar increase, 0.4 kcal mol$^{-1}$, is found when comparing PA with iPA, although the energy difference is within the combined uncertainty in the $E_a$ values. These results, taken together with the average energetic contribution of $>CH_2$ groups, indicate that methyl groups contribute, on average, 1.29 ± 0.20 kcal mol$^{-1}$ to the dissociation $E_a$ of the $(Lg + FA)_f^{7-}$ ions. The higher interaction energy of a $-CH_3$ group can be explained by its larger size and, consequently, greater polarizability, compared to a $>CH_2$ group. Inspection of the $E_a$ values (*fast* component) obtained for complexes containing the unsaturated forms of SA, with one, two, or three double bonds (i.e., SA-1, SA-2, or SA-3, respectively), reveals that unsaturation leads to a small but measurable increase in $E_a$, with each double bond contributing an additional 0.40 ± 0.01 kcal mol$^{-1}$ to $E_a$ (Figure 3). In other

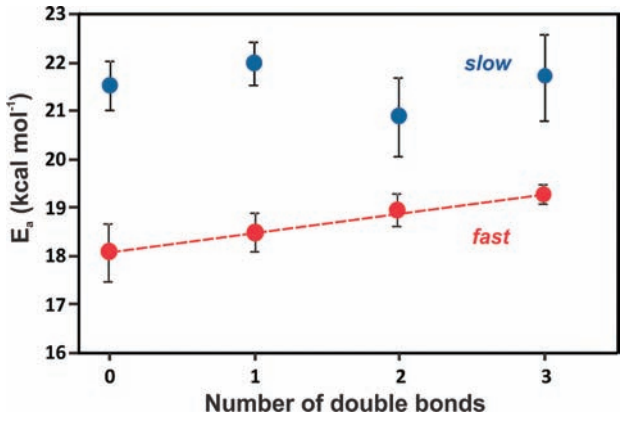


**Figure 3.** Plots of activation energies ($E_a$) measured for the dissociation of $(Lg + L)_f^{7-}$ (red circles) and $(Lg + L)_s^{7-}$ ions (blue circles), where L = SA, SA-1, SA-2, and SA-3, versus the number of double bonds in L. The dashed line corresponds to linear least-squares fit of the $E_a$ values determined for the $(Lg + FA)_f^{7-}$ ions.

words, each $-HC{=}CH-$ group contributes, on average, 2.04 ± 0.10 kcal mol$^{-1}$ to the dissociation $E_a$. The enhanced stability resulting from unsaturation of the acyl chain is attributed to the greater polarizabilty of the double bonds owing to the more delocalized $\pi$ bonding electrons.

It is interesting to note that the $E_a$ values measured for the *fast* components of the Lg complexes of RA and RO deviate from the trend established for the FAs (Figure 2). For an FA consisting of the same number of carbons, the dissociation $E_a$ for the *fast* component would be expected to be ~19 kcal mol$^{-1}$, significantly larger than the measured values of ~13 kcal mol$^{-1}$. The crystal structure reported for the (Lg + RA) complex[28] suggests an explanation for the lower $E_a$ values. According to the reported structure, RA is not fully buried inside the hydrophobic cavity of Lg (Supporting Information Figure S3a). Instead, only 12 of the carbons are well solvated by Lg. On the basis of the relationship between $E_a$ and size of the ligands (i.e., number of carbons) established above, the $E_a$ for such as structure would be expected to be ~12 kcal mol$^{-1}$, in agreement with the experimental values (12.6 ± 0.2 kcal mol$^{-1}$). These results suggest that, similar to the crystal structure, RA (and RO) is only partially solvated by Lg in the gas phase. The results of MD simulations performed on the gaseous $(Lg + RA)^{7-}$ ion also support the view, although some of the intermolecular contacts predicted from the simulations differ from those found in the crystal structure (Supporting Information Figure S3b).

**Comparison of $E_a$ Values with Hydrocarbon Transfer Enthalpies.** It is instructive to compare the energetic contributions that $-CH_3$, $>CH_2$, and $-HC{=}CH-$ groups make to the $E_a$ values for the dissociation of the gaseous (Lg +

$L)_f^{7-}$ ions with the contribution that these groups make to the change in enthalpy ($\Delta H_{v\rightarrow S}$) for the transfer of hydrocarbons from the gas phase to organic solvents. Listed in Table 2 are the

**Table 2. Comparison of the Average Contribution of $-CH_3$, $>CH_2$, and $-HC{=}CH-$ Groups to the Dissociation $E_a$ of the Gaseous $(Lg + L)_f^{7-}$ Ions and Their Average Contribution to the Negative Enthalpies of Transfer ($-\Delta H_{v\rightarrow S}$) of Hydrocarbons from the Gas Phase to Various Organic Solvents at 25 °C[a]**

| solvent | $-CH_3$ | | $>CH_2$ | $-HC{=}CH-$ |
|---|---|---|---|---|
| DMF (39) | – | | 0.89 ± 0.06[c] | 2.36 ± 0.28[d] |
| Methanol (32.6) | 1.06[b] | 1.06[b] | 0.98 ± 0.04[c] | 2.26 ± 0.14[d] |
| Acetone (20.7) | 1.19[b] | 0.88[b] | | (2.3)[e] |
| Hexane (1.9) | 1.07[b] | 1.33[b] | | |
| Cyclohexane (2.2) | 1.38[b] | 1.12[b] | 1.12 ± 0.02[c] | 2.12 ± 0.14[d] |
| Benzene (2.3) | 1.03[b] | 1.07[b] | 1.04 ± 0.04[c] | 2.44 ± 0.18[d] |
| 1-octanol (10.3) | 1.20[b] | 1.10[b] | 1.14 ± 0.03[c] | |
| 1-butanol (17.1) | 1.24[b] | 1.19[b] | 1.04 ± 0.03[c] | |
| Lg | 1.29 ± 0.20 | | 0.82 ± 0.04 | 2.04 ± 0.10 |

[a]Solvent dielectric constants ($\varepsilon$), at 25 °C, are shown in brackets. Errors correspond to one standard deviation. [b]Values taken from ref 25. [c]Values taken from ref 26. [d]Values taken from ref 24. [e]Value estimated based on dipole moments of DMF, methanol, and acetone.

average contributions of methylene groups to $\Delta H_{v\rightarrow S}$ reported by Abraham[25] and by Fuchs and Stephenson[26] for methanol, *N*,*N*-dimethylformamide (DMF), 1-butanol, 1-octanol, benzene, and cyclohexane. Also listed are values for acetone and hexane, as well as the average contributions of methyl groups to $\Delta H_{v\rightarrow S}$ for seven different solvents, reported by Abraham.[25] The contribution of $-HC{=}CH-$ groups in linear alkanes to $\Delta H_{v\rightarrow S}$ for DMF, methanol, cyclohexane, and benzene, as determined by Fuchs and co-workers,[24] are also listed in Table 2. Although no $\Delta H_{v\rightarrow S}$ value is available for the transfer of $-HC{=}CH-$ groups to acetone, the enthalpy change can be estimated based on a comparison of the dipole moments of acetone, methanol, and DMF. As discussed by Fuchs and co-workers,[24] the solvation of unsaturated hydrocarbons by polar solvents is expected to be dominated by dipole-induced dipole interactions, which in turn reflects the magnitude of the dipole moment. Given that the dipole moment of acetone (2.88) is in between the values for methanol (1.70) and DMF (3.82), it is reasonable to expect a $\Delta H_{v\rightarrow S}$ value that is in between that of methanol (2.26 kcal mol$^{-1}$) and DMF (2.36 kcal mol$^{-1}$), in other words a value of ~2.3 kcal mol$^{-1}$.

As noted above, the contribution that $-CH_3$ groups make to the $E_a$ values varies depending on their location on the acyl chain and, correspondingly, their location within the Lg cavity. However, the average interaction energy (1.29 ± 0.20 kcal mol$^{-1}$) is most similar to the $-\Delta H_{v\rightarrow S}$ value reported for 1-butanol (1.24 kcal mol$^{-1}$), which has a dielectric constant ($\varepsilon$) of 17.1 at 25 °C. The average interaction energy for $-HC{=}CH-$ groups with Lg in the gas phase (2.04 ± 0.10 kcal mol$^{-1}$) most closely resembles the $\Delta H_{v\rightarrow S}$ value reported for cyclohexane (2.12 kcal mol$^{-1}$), which is a nonpolar solvent with a $\varepsilon$ of 2.2. However, this comparison is complicated by the relatively small number of available $\Delta H_{v\rightarrow S}$ values and by the rather large uncertainties in the values. Comparison of the average interaction energy determined previously for methylene groups (0.82 ± 0.04 kcal mol$^{-1}$)[13] and the $\Delta H_{v\rightarrow S}$ values reveals that the solvation of the acyl chain $>CH_2$ groups in the Lg cavity is energetically comparable to that experienced in relatively polar solvents, such as acetone (0.88 kcal mol$^{-1}$) and DMF (0.89 kcal mol$^{-1}$), which have dielectric constants of 20.7 and 39, respectively.

The results of this analysis lead to several important conclusions. First, the interior of the Lg cavity does not provide a uniform solvent environment to the FA ligands and the exact nature of the environment, in terms of the energetics of the intermolecular interactions, differs for the different functional groups. Most importantly, the results of this study reveal that, for $-CH_3$ and $>CH_2$ groups, the interior of the cavity of Lg resembles a relatively polar solvent, with an apparent dielectric constant ≥17. These findings—a nonuniform solvent environment and high apparent dielectric constants—are consistent with those drawn from recent studies of the p$K_a$'s of ionizable groups within the hydrophobic interior of proteins.[29,30] For example, from the analysis of the shifts in the p$K_a$'s of 23 internal glutamic acid (Glu) residues of staphylococcal nuclease, compared to the normal p$K_a$ of Glu, apparent dielectric constants were established and found to range from 9 to 38.[30] Interestingly, no obvious correlation between the magnitude of the shift in p$K_a$ and location of the residue or proximity to other groups was found.[30] That independent experimental probes, gas phase dissociation energetics, and shifts in p$K_a$ values yield a consistent view of the environment within the hydrophobic interior of proteins is notable. Although the structural and physical origins of the high apparent dielectric constants values remain to be established, these findings argue for some refinement of the traditional view of hydrophobic protein–ligand binding and the nature of the environment within hydrophobic protein cavities.

**Are the Gas Phase Measurements Relevant to Protein–Ligand Binding in Water?** The $E_a$ values measured for the dissociation of the gaseous $(Lg + L)_f^{7-}$ ions provide unprecedented insight of the intrinsic energetics of protein–lipid interactions, and are, by themselves, of fundamental interest. However, it is relevant to ask whether the gas phase data are at all related to the stabilities of the (Lg + L) complexes in aqueous solution. To answer this question, we first compared the kinetic data measured for the gaseous $(Lg + L)_f^{7-}$ ions in the gas phase with the association free energies ($\Delta G_a$) measured for the (Lg + L) complexes in aqueous solution at 25 °C and pH 8.5 (Supporting Information Table S1). It can be seen from a plot of $-\Delta G_a$ versus $E_a$ (Figure 4a) that the solution and gas phase values are linearly correlated ($R^2$ = 0.97). Moreover, a plot of $-\Delta G_a$ versus the Gibbs free energy of activation ($\Delta G^{\ddagger}_g$) for dissociation of the gaseous $(Lg + L)_f^{7-}$ ions, calculated from the rate constants measured at 25 °C using the thermodynamic formulation of transition state theory, eq 2:

$$k = \frac{k_B T}{h} e^{-\Delta G^{\ddagger}/RT} \quad (2)$$

where $\Delta G^{\ddagger}_g$ is the Gibbs free energy of activation, $k_B$ is Boltzmann's constant, $h$ is Planck's constant, $R$ is the gas constant, and $T$ is the temperature, also reveals a linear correlation (Figure 4b).

The existence of linear correlations between the solution and gas phase data, which reflect the linear dependence of both the thermodynamic and kinetic parameters on the size (number of carbon atoms) of the FA ligands, represents compelling evidence that the intermolecular protein–lipid interactions in

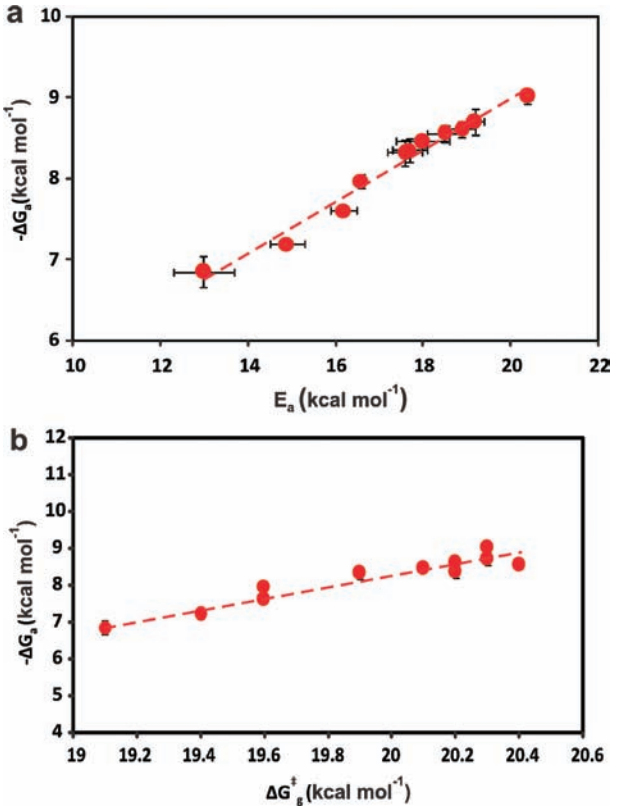


**Figure 4.** Plot of the negative Gibbs free energy of association ($-\Delta G_a$) in solution for the (Lg + L) complexes (pH 8.5 and 25 °C) versus (a) the activation energies ($E_a$) and (b) the free energies of activation ($\Delta G^{\ddagger}_g$) at 25 °C, measured in the gas phase for the dissociation of the $(Lg + L)_f^{7-}$ ions, where L = LA, MA, PA, SA, SA-1, SA-2, SA-3, iPA, 10-MePA, 15-MePA, and PhA.

the hydrated (Lg + L) complexes are generally preserved upon transfer from solution to the gas phase by ESI. Structural changes occurring in the gas phase, such as the formation of H-bonds between Lg and the ligand carboxyl group, result in a loss of correlation. This effect is evident from a comparison of the $E_a$ values determined for the $(Lg + L)_s^{7-}$ ions and the corresponding $\Delta G_a$ values (Supporting Information Figure S4).

It is worth noting that this is the first report of a protein–ligand binding system for which the gas phase dissociation kinetics and the $-\Delta G_a$ values in solution exhibit such correlation. This relationship can be exploited to estimate "effective" association constants ($K_a$) for ligands in cases where solution binding measurements are not easily performed. As an example, the dissociation $E_a$ for the $(Lg + L)_f^{7-}$ ion composed of retinol (RO), which is insoluble in water, was found to be identical (12.5 ± 0.4 kcal mol$^{-1}$), within experimental error, to the value measured for RA (12.6 ± 0.2 kcal mol$^{-1}$). On the basis of the arguments above, it can be concluded that Lg exhibits the same intrinsic $K_a$ for RO, as for RA, in water.

To further probe the relevance of the gas phase kinetic measurements to the stability of the (Lg + L) complexes in solution, $E_a$ values were determined for the dissociation of the (Lg + L) complexes, composed of iPA, 10-MetPA, and 15-MetPA, in aqueous solution at pH 8 using surface plasmon resonance spectroscopy. The Arrhenius parameters are listed in Table 3, along with the values previously reported for PA and SA.[23] In all cases, the $E_a$ values measured in solution are significantly smaller than the corresponding gas phase values.

**Table 3. Comparison of the Differences in the Dissociation Activation Energies ($\Delta E_a = E_{a,g} - E_{a,sol}$), Measured for the Gaseous $(Lg + L)_f^{7-}$ Ions ($E_{a,g}$) and the (Lg + L) Complexes in Aqueous Solution ($E_{a,sol}$) at pH 8, and the Hydration Enthalpies ($-\Delta H_{hydr}$) Calculated for the Ligand (L) Acyl Chains[a]**

| L | $E_{a,g}$ (kcal mol$^{-1}$) | $E_{a,sol}$ (kcal mol$^{-1}$) | $\Delta E_a$ (kcal mol$^{-1}$) | $-\Delta H_{hyd}$ (kcal mol$^{-1}$) |
|---|---|---|---|---|
| PA | 16.2 ± 0.3[b] | 5.5 ± 0.4[b] | 10.8 ± 0.5 | 11.7 |
| SA | 18.0 ± 0.6[b] | 6.0 ± 0.3[b] | 12.0 ± 0.7 | 13.1 |
| iPA | 16.6 ± 0.1 | 4.0 ± 0.5 | 12.6 ± 0.5 | 12.8–13.4 |
| 10-MePA | 17.7 ± 0.4 | 4.0 ± 0.3 | 13.7 ± 0.5 | 13.4–14.1 |
| 15-MePA | 17.6 ± 0.4 | 5.5 ± 0.3 | 12.1 ± 0.5 | 13.4–14.1 |

[a]The reported errors are one standard deviation. [b]Values taken from ref 23.

Recently, it was proposed that the differences in the $E_a$ values measured in gas phase (for the *fast* components) and in solution (i.e., $E_{a,g} - E_{a,sol} = \Delta E_a$) for PA and SA reflect the reduction in the energy barrier to ligand escape in solution due to the hydration of the exposed acyl chain in the *TS*.[23] Underlying this hypothesis is the assumption that the dissociation reactions of the hydrated and dehydrated complexes are mechanistically similar and involve a late *TS*, in which the ligand has almost fully escaped the cavity.[13,23] Support for this hypothesis was found in the quantitative agreement between the experimentally determined $\Delta E_a$ values and the hydration enthalpies calculated[25] for the corresponding $CH_3(CH_2)_x-$ groups of the FAs. A similar analysis was carried out using the kinetic data measured in the present study for iPA, 10-MetPA, and 15-MetPA. Calculation of the $\Delta H_{hydr}$ values in the case of branched FAs is complicated by the absence of tabulated hydration values for >CH– groups. To deal with this deficiency, $\Delta H_{hydr}$ values were calculated in two different ways, (1) treating >CH– groups as being equivalent to $>CH_2$ groups and (2) neglecting the >CH– group from the calculation. The former approach is expected to lead to a slight overestimation of the actual $\Delta H_{hydr}$ values, while the latter approach should lead to a slight underestimation. Notably, the $\Delta E_a$ values determined for the iPA and 10-MetPA fall within the range of $\Delta H_{hydr}$ values, while the $\Delta E_a$ value for 15-MetPA is ~1 kcal mol$^{-1}$ smaller than the $\Delta H_{hydr}$ value calculated by neglecting the >CH– group (Table 3). The modest uncertainty in the magnitude of the $\Delta H_{hydr}$ values notwithstanding, the similarity in the $\Delta E_a$ and $\Delta H_{hydr}$ values for these five ligands provides additional support to the hypotheses that the dissociation of the solvated and desolvated (Lg + L) complexes share similar mechanisms, both involving a late *TS*, and that the differences in the $E_a$ values measured in the gas phase and in solution arise predominantly from the hydration of the acyl chain of L in the *TS*.

## ■ CONCLUSIONS

This study has produced a number of important findings. First, clear relationships between the dissociation kinetics and activation energies measured for the deprotonated ions of the (Lg + L) complexes in the gas phase and their thermodynamic and kinetic stabilities in aqueous solution were established. To our knowledge, this is the first protein–ligand system for which such relationships have been identified. These relationships represent compelling evidence that the solvated and desolvated

(Lg + L) complexes share similar protein−lipid interactions. These results also argue for similar dissociation mechanisms, both involving a late *TS*, operating in solution and the gas phase. Most importantly, the intrinsic energetic contributions of $-CH_3$, $>CH_2$, and $-HC{=}CH-$ groups to protein−lipid interactions were evaluated for the first time. Comparison of the energetic data with enthalpies for the transfer of hydrocarbons from the gas phase to organic solvents reveals that, for $-CH_3$ and $>CH_2$ groups, the interior of the cavity of Lg resembles a relatively polar solvent, with an apparent dielectric constant ≥17.

## ■ ASSOCIATED CONTENT

### Supporting Information

Thermodynamic and kinetic data, and results of MD simulations. This material is available free of charge via the Internet at http://pubs.acs.org.

## ■ AUTHOR INFORMATION


### Corresponding Author

john.klassen@ualberta.ca


## ■ ACKNOWLEDGMENTS

The authors are grateful for financial support provided by the Natural Sciences and Engineering Research Council of Canada (NSERC) and the Alberta Glycomics Centre.

## ■ REFERENCES


(1) Tanford, C. *Science* **1978**, *200*, 1012−1018.

(2) Tanford, C. *Protein Sci.* **1997**, *6*, 1358−1366.

(3) (a) Pace, C. N.; Shirley, B. A.; McNutt, M.; Gajiwala, K. *FASEB J.* **1996**, *10*, 75−83. (b) Efremov, R. G.; Chugunov, A. O.; Pyrkov, T. V.; Priestle, J. P.; Arseniev, A. S.; Jacoby, E. *Curr. Med. Chem.* **2007**, *14*, 393−415. (c) Meyer, E. E.; Rosenberg, K. J.; Israelachvili, J. *Proc. Natl. Acad. Sci. U.S.A.* **2006**, *103*, 15739−15746.

(4) Southall, N. T.; Dill, K. A.; Haymet, A. D. *J. Phys. Chem. B.* **2002**, *106*, 521−533.

(5) (a) Lazaridis, T. *Acc. Chem. Res.* **2001**, *34*, 931−937. (b) Southall, N. T.; Dill, K. A. *J. Phys. Chem. B* **2000**, *104*, 1326−1331.

(6) (a) Mondal, J.; Yethiraj, A. *J. Phys. Chem. Lett.* **2011**, *2*, 2391−2395. (b) Snyder, P. W.; Mecinović, J.; Moustakas, D. T.; Thomas, S. W. III; Harder, M.; Mack, E. T.; Lockett, M. R.; Héroux, A.; Sherman, W.; Whitesides, G. M. *Proc. Natl. Acad. Sci. U.S.A.* **2011**, *108*, 17889−17894. (c) Varilly, P.; Patel, A. J.; Chandler, D. J. *Chem. Phys.* **2011**, *134*, 074109. (d) Dill, K. A.; Truskett, T. M.; Vlachy, V.; Hribar-Lee, B. *Annu. Rev. Biophys. Biomol. Struct.* **2005**, *34*, 173−199.

(7) Dill, K. A. *J. Biol. Chem.* **1997**, *272*, 701−704.

(8) Loo, J. A. *Mass Spectrom. Rev.* **1997**, *16*, 1−23.

(9) Li, Y.; Heitz, F.; Grimellec, C. L.; Cole, R. B. *Anal. Chem.* **2005**, *77*, 1556−1565.

(10) Stanley, W. A.; Versluis, K.; Schultz, C.; Heck, A. J. R.; Wilmanns, M. *Arch. Biochem. Biophys.* **2007**, *461*, 50−58.

(11) Barrera, N. P.; Bartolo, N. D.; Booth, P. J.; Robinson, C. V. *Science* **2008**, *321*, 243−246.

(12) Uetrecht, C.; Barbu, I. M.; Shoemaker, G. K.; van Duijn, E.; Heck, A. J. R. *Nat. Chem.* **2011**, *3*, 126−132.

(13) Liu, L.; Bagal, D.; Kitova, E. N.; Schnier, P. D.; Klassen, J. S. *J. Am. Chem. Soc.* **2009**, *131*, 15980−15981.

(14) (a) Sun, J.; Kitova, E. N.; Klassen, J. S. *Anal. Chem.* **2007**, *79*, 416−425. (b) Bagal, D.; Kitova, E. N.; Liu, L.; El-Hawiet, A.; Schnier, P. D.; Klassen, J. S. *Anal. Chem.* **2009**, *81*, 7801−7806.

(15) (a) Benesch, J. L. P.; Sobott, F.; Robinson, C. V. *Anal. Chem.* **2003**, *75*, 2208−2214. (b) Loo, J. A.; He, J. X.; Cody, W. L. *J. Am. Chem. Soc.* **1998**, *120*, 4542−4543. (c) Rostom, A. A.; Fucini, P.; Benjamin, D. R.; Juenemann, R.; Nierhaus, K. H.; Hartl, F. U.; Dobson, C. M.; Robinson, C. V. *Proc. Natl. Acad. Sci. U.S.A.* **2000**, *97*, 5185−5190. (d) van Duijn, E.; Simmons, D. A.; van den Heuvel, R. H.; Bakkes, P. J.; van Heerikhuizen, H.; Heeren, R. M.; Robinson, C. V.; van der Vies, S. M.; Heck, A. J. *J. Am. Chem. Soc.* **2006**, *128*, 4694−4702. (e) van den Heuvel, R. H. H.; van Duijn., E.; Mazon, H.; Synowsky, S. A.; Lorenzen, K.; Versluis, C.; Brouns, S. J. J.; Langridge, D.; van der Oost, J.; Hoyes, J.; Heck, A. J. R. *Anal. Chem.* **2006**, *78*, 7473−7483. (f) Wu, Q. Y.; Gao, J. M.; Joseph-McCarthy, D.; Sigal, G. B.; Bruce, J. E.; Whitesides, G. M.; Smith, R. D. *J. Am. Chem. Soc.* **1997**, *119*, 1157−1158. (g) Benesch, J. L. P.; Aquilina, J. A.; Ruotolo, B. T.; Sobott, F.; Robinson, C. V. *Chem. Biol.* **2006**, *13*, 597−605.

(16) (a) Shelimov, K. B.; Clemmer, D. E.; Hudgins, R. R.; Jarrold, M. F. *J. Am. Chem. Soc.* **1997**, *119*, 2240−2248. (b) Robinson, E. W.; Leib, R. D.; Williams, E. R. *J. Am. Soc. Mass Spectrom.* **2006**, *17*, 1469−1479. (c) Koeniger, S. L.; Merenbloom, S. I.; Sevugarajan, S.; Clemmer, D. E. *J. Am. Chem. Soc.* **2006**, *128*, 11713−11719. (d) Ruotolo, B. T.; Giles, K.; Campuzano, I.; Sandercock, A. M.; Bateman, R. H.; Robinson, C. V. *Science* **2005**, *310*, 1658−1661. (e) Bleiholder, C.; Dupuis, N. F.; Wyttenbach, T.; Bowers, M. T. *Nat. Chem.* **2011**, *3*, 172−177.

(17) (a) Oomens, J.; Polfer, N.; Moore, D. T.; van der Meer, L.; Marshall, A. G.; Eyler, J. R.; Meijer, G.; von Helden, G. *Phys. Chem. Chem. Phys.* **2005**, *7*, 1345−1348. (b) Compagnon, I.; Oomens, J.; Meijer, G.; von Helden, G. *J. Am. Chem. Soc.* **2006**, *128*, 3592−3597. (c) Iavarone, A. T.; Parks, J. H. *J. Am. Chem. Soc.* **2005**, *127*, 8606−8607.

(18) Wu, S.-Y.; Perez, M. D.; Puyol, P.; Sawyer, L. *J. Biol. Chem.* **1999**, *274*, 170−174.

(19) (a) Kontopidis, G.; Holt, C.; Sawyer, L. *J. Dairy Sci.* **2004**, *87*, 785−796. (b) Qin, B. Y.; Bewley, M. C.; Creamer, L. K.; Baker, H. M.; Baker, E. N.; Jameson, G. B. *Biochemistry* **1998**, *37*, 14014−14023.

(20) Qvist, J.; Davidovic, M.; Hamelberg, D.; Halle, B. *Proc. Natl. Acad. Sci. U.S.A.* **2008**, *105*, 6296−6301.

(21) (a) Kontopidis, G.; Holt, C.; Sawyer, L. *J. Dairy Sci.* **2004**, *87*, 785−796. (b) Collini, M.; D'Alfonso, L.; Molinari, H.; Ragona, L.; Catalaono, M.; Baldini, G. *Protein Sci.* **2003**, *12*, 1596−1603. (c) Konuma, T.; Sakurai, K.; Goto, Y. *J. Mol. Biol.* **2007**, *368*, 209−218.

(22) Liu, L.; Kitova, E. N.; Klassen, J. S. *J. Am. Soc. Mass Spectrom.* **2011**, *22*, 310−318.

(23) Liu, L.; Michelsen, K.; Kitova, E. N.; Schnier, P. D.; Klassen, J. S. *J. Am. Chem. Soc.* **2010**, *132*, 17658−17660.

(24) Saluja, P. P. S; Young, T. M.; Rodewald, R. F.; Fuchs, F. H.; Kohli, D.; Fuchs, R. *J. Am. Chem. Soc.* **1977**, *99*, 2949−2953.

(25) Abraham, M. H. *J. Am. Chem. Soc.* **1982**, *104*, 2085−2094.

(26) Fuchs, R.; Stephenson, W. K. *Can. J. Chem.* **1985**, *63*, 349−352.

(27) Spirin, S.; Titov, M.; Karyagina, A.; Alexeevski, A. *Bioinformatics* **2007**, *23*, 3247−3248.

(28) Kontopidis, G.; Holt, C.; Sawyer, L. *J. Mol. Biol.* **2002**, *318*, 1043−1055.

(29) Dwyer, J. J.; Gittis, A. G.; Karp, D. A.; Lattman, E. E.; Spencer, D. S.; Stites, W. E.; Garcia-Moreno, B. E. *Biophys. J.* **2000**, *79*, 1610−1620.

(30) Isom, D. G.; Castaneda, C. A.; Cannon, B. R.; Velu, P. D.; Garcia-Moreno, B. E. *Proc. Natl. Acad. Sci. U.S.A.* **2010**, *107*, 16096−16100.